Fault Heterogeneity and the Connection between Aftershocks and Afterslip

Eugenio Lippiello, Giuseppe Petrillo, François Landes, Alberto Rosso

Bulletin of the Seismological Society of America, Vol. , No. , pp. –, , doi: 10.1785/0120180244

Short Note

Fault Heterogeneity and the Connection between Aftershocks and Afterslip

by E. Lippiello, G. Petrillo, F. Landes,* and A. Rosso

Abstract Whether aftershocks originate directly from the mainshock and surrounding stress environment or from afterslip dynamics is crucial to the understanding of the nature of aftershocks. We build on a classical description of the fault and creeping regions as two blocks connected elastically, subject to different friction laws. We show analytically that, upon introduction of variability in the fault plane's static friction threshold, a nontrivial stick-slip dynamics ensues. In particular, we support the hypothesis (Perfettini and Avouac, 2004) that the aftershock occurrence rate is proportional to the afterslip rate, up to a corrective factor that is also computed. Thus, the Omori law originates from the afterslip's logarithmic evolution in the velocity-strengthening region. We confirm these analytical results with numerical simulations, generating synthetic catalogs with statistical features in good agreement with instrumental catalogs. In particular, we recover the Gutenberg–Richter law with a realistic b-value ($b \simeq 1$) when Coulomb stress thresholds obey a power-law distribution.

Introduction

A mainshock is followed by the increase of seismic activity caused by aftershocks as well as by a significant time-dependent postseismic deformation known as afterslip. The common interpretation is that afterslip is activated by the stress increase due to the mainshock's coseismic instantaneous deformation and mostly occurs in regions with a velocity-strengthening rheology. This interpretation dates back to the seminal paper by Marone *et al.* (1991) who analytically obtained a hyperbolic time decay of the postseismic deformation rate $\dot{u}(t) \sim 1/t$, for a velocity-strengthening region. The hyperbolic temporal decay is similar to the one usually observed for the aftershock occurrence rate $\lambda(t)$

$$\lambda(t) = \frac{K}{t + c}, \tag{1}$$

and known as the Omori law.

The proportionality between aftershock occurrence rate $\lambda(t)$ and stress or strain rate $\dot{u}(t)$ has been documented by the postseismic deformation measured after several large earthquakes (Perfettini and Avouac, 2004, 2007; Perfettini *et al.*, 2005, 2018; Hsu *et al.*, 2006; Perfettini and Ampuero, 2008; Savage and Yu, 2007; Savage and Langbein, 2008; Savage, 2010; Canitano *et al.*, 2018). Perfettini and Avouac (2004) explained the observed proportionality under the assumption that aftershocks are induced by afterslip. This result was supported by the analytical solution of a single spring-slider model under velocity-strengthening friction, which models brittle creeping. The proportionality has been also used to obtain the friction parameters as well as the stressing rate, in a given velocity-strengthening region, from the temporal behavior of the recorded aftershocks (Frank *et al.*, 2017).

In this short note, we present a minimal model of the fault as a sliding block connected to the afterslip region treated, as in Marone *et al.* (1991) and Perfettini and Avouac (2004), as a second block with velocity-strengthening rheology (see Fig. 1). In this two-block model, the slip of the fault block induces the afterslip relaxation of the second block, which in turns promotes further failures of the fault. The central assumption is that instability thresholds f^{th}, on the fault plane, are not uniform but random with a distribution $g(f^{th})$. This makes more realistic the description of the fault as a single-slider block. Previous studies (Kaneko and Lapusta, 2007; Ader *et al.*, 2014), indeed, have shown that the absence of heterogeneities is responsible for important differences between single-slider models and 2D continuum models. The presence of random thresholds allows us to analytically demonstrate that, without any assumption on the initial stress distribution, the proportionality $\lambda(t) \propto \dot{u}(t)$ is a stable feature of earthquake triggering. We present analytical and numerical results of the model evolution.

*Also at Department of Physics and Astronomy, University of Pennsylvania, Philadelphia, Pennsylvania U.S.A.; and Department of Chemistry, Columbia University, New York, New York 10027 U.S.A.

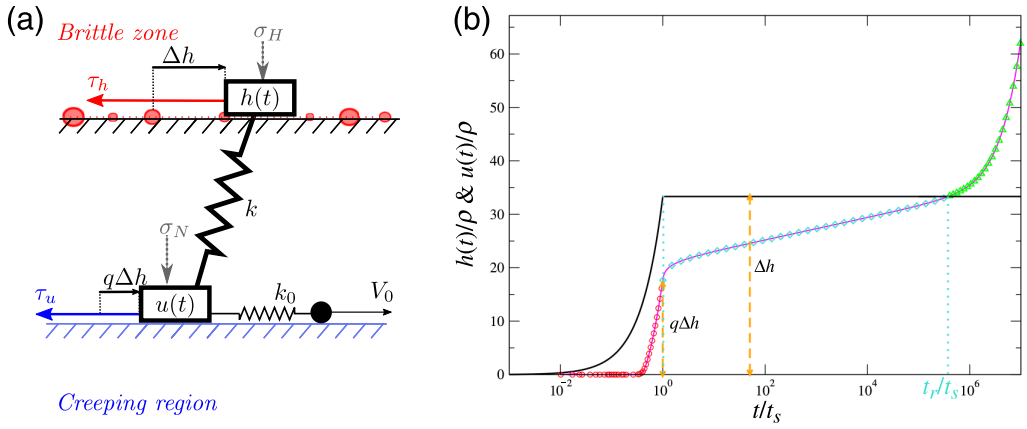

Figure 1. (a) The two block model. The block H, at the position $h(t)$, represents the fault, which performs discrete jumps of fixed amplitude Δh and can be stuck in different positions indicated by dots. The size of each dot represents the local value of f^{th}. The block U, at the position $u(t)$, is subject to a velocity-strengthening friction and is driven at a constant rate $k_0 V_0$. Both blocks are subject to confining pressures σ_N and σ_H. The exact solution of equation (3) assuming the slip starts at $t = 0$ and ends at $t = t_s$ with the block H moving at a constant velocity V_S. Distances are expressed in units of ρ and time in unit of t_s. We use $\Delta h = 33\rho$, $V_0 = 10^{-5}\delta h/t_s$, and $k/k_0 = 33$. The fault displacement $h(t)/\rho$ is plotted with a continuous black line, whereas the full analytical solution of equation (3) for $u(t)/\rho$ is represented by a continuous gray line. Different colors and symbols indicate the evolution of $u(t)$ in the three regimes: circles (slip regime), diamonds (afterslip regime), and triangles (interseismic regime). The color version of this figure is available only in the electronic edition.

The Model

We describe the fault as a block H coupled by means of a spring of elastic coupling k to a second block U, which represents the creeping region of the crust, with velocity-strengthening friction. Marone *et al.* (1991) identified the region where afterslip occurs in a zone of unconsolidated sediments above the fault, whereas Perfettini and Avouac (2004, 2007) and Perfettini *et al.* (2005) assumed the creeping region zone to be deeper because of the transition toward ductile behavior caused by the increase of temperature with depth. In other studies, afterslip has been observed very close (Crescentini *et al.*, 1999), or even on the fault within the seismogenic zone (Miyazaki *et al.*, 2004; Johnson *et al.*, 2006; Freed, 2007). In our approach, the precise position of the velocity-strengthening region is not relevant and we assume that the block U is embedded in a more extensive region creeping at a constant velocity V_0. We model this interaction with a second spring of elastic constant k_0 whose free end moves with velocity V_0 (Fig. 1). To simplify the model, we assume that both blocks move in the V_0 direction, and therefore, only scalar quantities can be considered. Indicating with $u(t)$ and $h(t)$, the positions of the block U and the block H at the time t, respectively, the shear stress acting on U is $k(h(t) - u(t)) + k_0(V_0 t - u(t))$ and the friction force $\tau_u(t)$, under steady-state condition, can be written as

$$\tau_u(t) = \sigma_N\left(\mu_c + A\log\left(\frac{\dot{u}(t)}{V_c}\right)\right), \qquad (2)$$

in which $\dot{u}(t)$ is the block velocity, σ_N is the effective normal stress, μ_c is the static friction coefficient when the block U slides at the steady velocity V_c and $A > 0$ for a velocity-strengthening material. In the overdamped limit, the constitutive equation for U reads

$$\tau_u(t) = k(h(t) - u(t)) + k_0(V_0 t - u(t)), \qquad (3)$$

which admits a stationary solution for $\dot{u}(t) = V_c = \frac{k_0}{k_0+k}V_0$. In general, one has

$$\dot{u}(t) = V_c \exp\left(\frac{h(t)}{\rho} + \frac{t}{t_R} - \frac{\mu_c}{A} - \frac{u(t)}{\rho_0}\right), \qquad (4)$$

in which $\rho_0 = \frac{A\sigma_N}{k+k_0}$ and $\rho = \frac{A\sigma_N}{k}$ are two characteristic length, whereas $t_R = \frac{A\sigma_N}{k_0 V_0} = \frac{\rho_0}{V_c}$ represents the long timescale associated with the extended creeping region at velocity V_0.

We next consider the evolution of the block U starting from the stationary solution $\dot{u}(0) = V_c$ at the time $t = 0$. The solution for $u(t)$ was written in Perfettini and Avouac (2004) in terms of the evolution of $h(t)$:

$$u(t) = u(0) + \rho_0 \log\left(1 + \frac{1}{t_R}F(t)\right)$$
$$F(t) = \int_0^t \exp\left(\frac{t'}{t_R} + \frac{(h(t') - h(0))}{\rho}\right)dt'. \qquad (5)$$

Concerning the dynamics of the block H, we assume the Coulomb failure criterion (CFC): the instability is only controlled by the Coulomb stress $S_H(t)$ acting at time t on the block H, with $S_H(t) = k(u(t) - h(t)) - \mu_H\sigma_H(t)$. Here $k(u(t) - h(t))$ is the shear stress, μ_H is a friction coefficient and $\sigma_H(t)$ is the effective normal stress represented by the normal stress reduced by the pore pressure. According to the CFC, under the assumption that $\sigma_H(t)$ is constant, the block H is unstable as soon as the shear stress overcomes

a reference frictional stress f^{th}. Treating each slip as instantaneous implies that H either is at rest or it slips in an infinitely short time. This approximation corresponds to a vanishing nucleation size coherently with the steady-state approximation in the constitutive equation (equation 3) (Rice and Ben-Zion, 1996). Within our hypothesis, the dynamics of the two blocks can be written in terms of the equation (5) and split in three regimes:

- *Slip Regime*: If at time $t = 0$, $k(u(0) - h(0)) > f^{th}$, the position of the block H becomes unstable and jumps of Δh inducing the coslip of the block U, which depends on the precise dynamics of the block H. For example in Figure 1, we present an explicit solution when $h(t)$ moves steadily at velocity $V_s \gg V_0$ for a short time t_s. In all cases, the block U slips coseismically with the block H of an amount $q\Delta h$ with $q \in [0, 1]$, so that the slip is given by

$$h(0) \to h(0) + \Delta h \tag{6}$$

$$u(0) \to u(0) + q\Delta h. \tag{7}$$

The precise value of q is a complicated function of model parameters and of the specific slip profile. In our minimal model, we assume that q is a fixed value equal for all slips. At the end of the slip, the block H experiences a stress drop $k(1 - q)\Delta h$, and if $k(u(t_s) - h(t_s)) < f^{th}$ the fault is stuck again $h(t) = h(t_s)$. In the hypothesis of a uniform frictional stress f^{th}, the fault exhibits a trivial dynamics characterized by jumps of equal size (Δh) separated by a constant time interval. In this case, the prestress value $f^{th} - k(u(0) - h(0))$ is peaked at a characteristic value and stress and seismic rate are not proportional. Nevertheless, different sources of heterogeneity should affect the local value of the friction coefficient: the presence of asperities, which induces fluctuations in the normal and pore pressure values, the variation of the basal friction coefficient, or again, the fluctuations of A. These parameters are temperature and water dependent and are likely to vary along the fault. Thus, it is reasonable that the frictional stress experienced after a slip Δh is typically different from the previous one (see the variable intensity of pinning points in Fig. 1, dots). Concretely, after each slip it is reasonable that the block H comes up against a new value of $f^{th} = f_1^{th}$ extracted from a distribution $g(f^{th})$ with a finite probability that $k(u(t_s) - h(t_s)) > f_1^{th}$. Hence, the block is still unstable and accordingly can perform n subsequent slips until the distance to failure $\delta F_h = f_n^{th} - k(u(0) - h(0)) - n(1 - q)\Delta h > 0$. In this case, the slip instability corresponds to a single slip of size $n\Delta h$ (a single earthquake) and the dynamics is characterized by earthquakes of different sizes. Large earthquakes can be, therefore, viewed as a succession of smaller seismic ruptures. After the slip, the block H is stuck in the novel position $h(t) = h(0) + n\Delta h$ and the evolution of $u(t)$ is given by the explicit solution of equation (5):

$$F(t) = t_R e^{\frac{n\Delta h}{\rho}} \left(e^{\frac{t}{t_R}} - 1 \right), \tag{8}$$

$$u(t) = u(0) + nq\Delta h + \rho_0 \log\left(1 + e^{\frac{n\Delta h}{\rho}} \left(e^{\frac{t}{t_R}} - 1 \right)\right). \tag{9}$$

Two distinct regimes can be identified.

- *Afterslip Regime*: At times shorter than t_R, one can replace $t_R(e^{\frac{t}{t_R}} - 1) \simeq t$ so that

$$u(t) = u(0) + nq\Delta h + \rho_0 \log\left(1 + \frac{e^{\frac{n\Delta h}{\rho}}}{t_R} t\right). \tag{10}$$

In this regime, the motion of U increases the stress on H inducing further slips of the block H, that is, the aftershocks. This occurs if $k\rho_0 \log(1 + \frac{e^{\frac{n\Delta h}{\rho}}}{t_R} t_{AS}) = \delta F_h$, namely

$$t_{AS} = \frac{t_R}{e^{\frac{n\Delta h}{\rho}}} \left(e^{\frac{\delta F_h}{k\rho_0}} - 1 \right) \quad \text{with} \quad t_{AS} \ll t_R. \tag{11}$$

- *Interseismic Regime*: At $t > t_R$, the motion of the block U is dominated by the creeping velocity V_0. In this regime, one can assume $(e^{\frac{t}{t_R}} - 1) \simeq e^{\frac{t}{t_R}}$ and neglect the one in the logarithm of equation (10). We obtain that the block U slides at the steady velocity $V_c = \frac{k_0}{k + k_0} V_0$:

$$u(t) = V_c t + \text{const}. \tag{12}$$

Statistics of Slip Events: Analytical Results

In the following, we explore the statistical features of the evolution of a single fault represented by the block H which, because of the coupling with the block U, can experience multiple slip events. The statistics of the single fault is expected to be representative of the statistics of a population of faults with random initial stress conditions.

The block H exhibits a stick-slip dynamics with nontrivial temporal correlations for a sufficiently broad distribution $g(f)$, which leads to a broad distributed distance to the next instability. In particular, we indicate with $t_0 = 0$ the time of the last slip and consider the probability $P_0(t)$ of no slip up to time t. Because $u(t)$ is monotonically increasing with time (equation 5), $P_0(t)$ corresponds to the probability to extract a friction threshold f_1^{th} larger than $k(u(t) - h(t))$, $P_0(t) = \int_{k(u(t)-h(t))}^{\infty} g(f) df$. In the hypothesis that $g(f)$ does not present sharp discontinuities, the evolution of the block H can be described as a time-dependent nonhomogeneous Poisson process with $P_0(t) = \exp(-\int_0^t \lambda(t') dt')$, in which $\lambda(t)$ is the seismicity rate, that is, the number of earthquake for unit time triggered by the mainshock. As a consequence, $\lambda(t) = -\frac{\partial \log(P_0(t))}{\partial t}$ leading to

$$\lambda(t) = Q(k(u(t) - h(t)))k\frac{\partial(u(t) - h(t))}{\partial t} \tag{13}$$

with

$$Q(x) = \frac{g(x)}{\int_x^\infty g(f)df}. \tag{14}$$

Taking into account that $h(t) = \text{const}$, outside the very short slip regime, we find

$$\lambda(t) = Q(k(u(t) - h(t)))k\dot{u}(t). \tag{15}$$

Because of the presence of the time-dependent coefficient $Q(k(u(t) - h(t)))$, equation (15) shows that in our model the seismic rate $\lambda(t)$ is not exactly proportional to the stress rate. However, we argue that in the afterslip regime $Q(k(u - h))$ can only depend logarithmically on time and the proportionality between aftershock and stress rate is, at first order, satisfied. More precisely, we first focus on three types of distributions for the friction thresholds: a Gaussian distribution $g(f) = \sqrt{\frac{\alpha}{\pi}}\exp(-\alpha(f - f_0)^2)$ restricted to positive f, a power-law distribution $g(f) = \frac{(\beta-1)f_0^{\beta-1}}{(f+f_0)^\beta}$ and an exponential distribution $g(f) = \frac{1}{\gamma}\exp(-\gamma f)$. In the case of the exponential distribution, $Q(k(u - h))$ is exactly a constant, whereas it displays logarithmic time dependence for the power law $(Q(k(u - h)) \sim 1/(k(u - h)) \sim 1/\log(t))$ and for the Gaussian distribution $(Q(k(u - h)) \sim k(u - h) \sim \log(t))$. Therefore, using $\frac{\partial k(u-h)}{\partial t} = k\dot{u}(t) \sim 1/t$ in the afterslip regime (equation 10), we always obtain the Omori hyperbolic decay $\lambda(t) \sim \dot{u} \sim 1/t$, with possible logarithmic corrections coming from $Q(t)$. An important exception to this behavior is represented by the distributions with an upper cutoff $f_{\max}$. In this case, one can easily derive (e.g., by considering the uniform distribution $[0, f_{\max}]$) that $Q(k(u - h)) \propto 1/(f_{\max} - k(u(t) - h(t)))$, which can diverge at finite time. Our results then shows that the key ingredients for the Omori law are represented by heterogeneities in the frictional stress values combined with the logarithmic stress relaxation induced by the velocity-strengthening rheology. This behavior is very general provided that the maximal values of the frictional stress are large compared to the increase of the stress that can be experienced during the afterslip phase.

The presence of frictional heterogeneities also produces a nontrivial slip-size distribution $p(n)$, which corresponds to the probability that the fault H performs a slip of size $n\Delta h$. Assuming a small stress drop $k(1 - q)\Delta h$ and the independence between subsequent jumps, we can use the mapping to a record problem. More precisely, we neglect the stress change after each slip assuming $k(u(t) - h(t)) - k(1 - q)\Delta h \simeq k(u(t_0) - h(t_0))$, and calculate $p(n)$ as the probability to draw $n + 1$ independent and identically distributed random variables $f_0^{th}, f_1^{th}, \ldots, f_n^{th}$, such that $f_j^{th} < f_0^{th}$ for $j \in [1, n - 1]$ and $f_n^{th} > f_0^{th}$. In this case, we find $p(n) \propto 1/(n^2 + n)$ for any probability density function $g(f_0)$ and independently of its domain $(f_{\min}, f_{\max})$ (here we assumed $f_{\min} \geq 0$ and $f_{\max} = \infty$). To show it, we remark $p(n) = \int_{f_{\min}}^{f_{\max}} df_0 g(f_0)$ $(P_<(f_0))^{n-1} \times P_>(f_0)$, in which $P_<(f_0) = \int_{f_{\min}}^{f_0} df' g(f')$ is the probability to draw a threshold smaller than f_0 and, similarly, $P_>(f_0) = 1 - P_<(f_0)$, which gives $g(f_0) = \frac{dP_<(f_0)}{df_0}$. As a consequence, $p(n) = \int_{f_{\min}}^{f_{\max}} df_0 \frac{dP_<(f_0))}{df}$ $((P_<(f_0))^{n-1} - (P_<(f_0))^n) = \frac{1}{n} - \frac{1}{n+1}$. For sufficiently large n, we obtain the power-law behavior $p(n) \sim n^{-\eta}$ with $\eta = 2$. This is in qualitative agreement with the Gutenberg–Richter (GR) law for the magnitude distribution. Indeed, taking into account that the size of a slip $n\Delta h$ is proportional to the seismic moment released during a slip instability, the GR law combined with the logarithmic relation between magnitude and seismic moment corresponds to a power-law behavior $p(n) \sim n^{-\eta}$ with $\eta = 1 + (2/3)b$, in which $b \simeq 1$ is the coefficient of the GR law.

Numerical Results

In numerical simulations, the block H is at rest at time t_0. We consider $k(u(t_0) - h(t_0)) < f^{th}$ and $u(t)$ evolving according to equation (12) which corresponds to the interseismic regime. The evolution of the block U increases the shear stress $\tau_h(t)$ and the first slip occurs at the time $t_0 + t_M$ with

$$t_M = \frac{1}{kV_c}\delta F_h = t_R\frac{\delta F_h}{k\rho_0} \tag{16}$$

obtained by the inversion of equation (12). The block H, then performs n subsequent slips before reaching the stable condition $\tau_h^{(n)} < f_n^{th}$, which corresponds to an earthquake of size $n\Delta h$ occurred at the time $t_0 + t_M$. The subsequent slip will occur at a time $t_0 + t_M + \delta t$, in which δt is the minimum between t_{AS} and t_M given by equations (11) and (16), respectively. If $\delta t = t_{AS}$, the new slip is correlated to the first one and they are considered belonging to the same seismic sequence. The process is iterated and therefore the sequence can contain many correlated earthquakes. A new sequence starts as soon as $\delta t = t_M$. In numerical simulations, we fix the value $\Delta h = 10\rho$ to have a clear time separation between t_{AS} and t_M (equations 11 and 16) and vary the only the g-related parameters $\alpha, \beta, \gamma, f_0$.

A typical numerical sequence is plotted in Figure 2a, where each point corresponds to an event with occurrence time t and size $n\Delta h$. The presence of correlated sequences, that is, the clusters, is manifest. In the majority of cases (more than 70%), the first event of the cluster is also the largest event belonging to the same sequence (Fig. 2c). In the remaining sequences, the largest event, the mainshock, is anticipated by few smaller events, the foreshocks (Fig. 2b).

In equation (11), we define aftershocks as those events following the first event of the sequence. In the following, we adopt the more standard definition as those events following

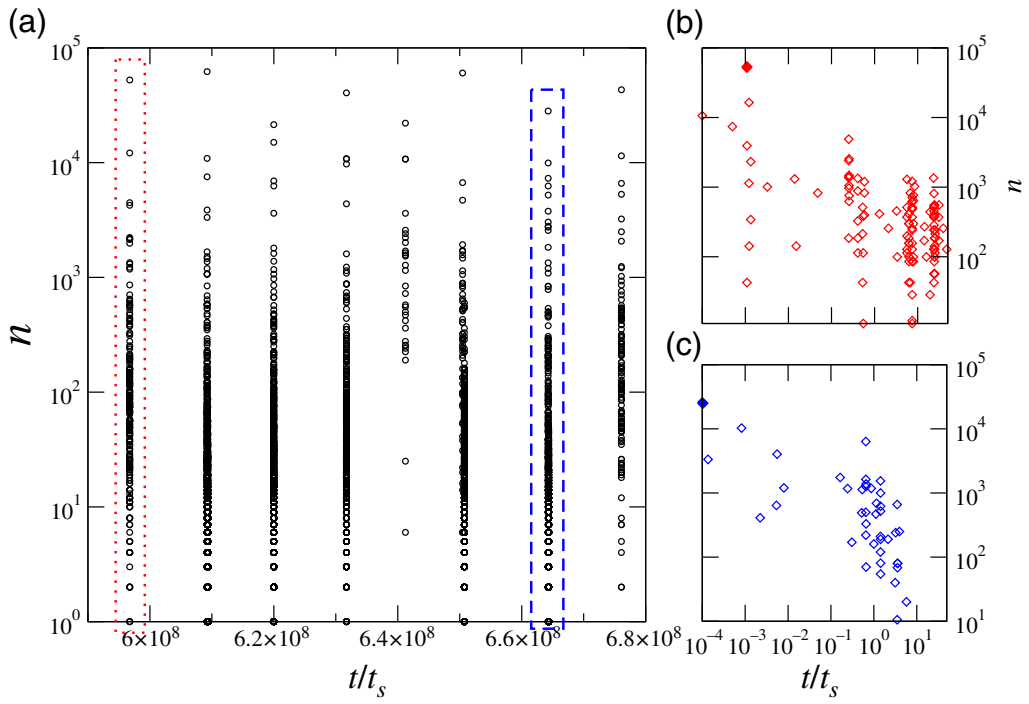

Figure 2. (a) A typical numerical catalog with a power-law-distributed $g(f)$ with, $\beta = 5$, $f_0 = 10$, and $\Delta h/\rho = 10$. (b) Zoom inside the temporal regions inside the dotted rectangle to show the mainshock–aftershock sequences with two foreshocks. Time has been shifted to have the first event of the sequence at the time $t = 10^{-4}t_s$. The mainshock is indicated by a filled symbol. (c) As for (b) for the region inside the dashed rectangle, corresponding to a sequence without foreshocks. The color version of this figure is available only in the electronic edition.

the mainshock. Because the number of foreshocks is always much smaller than the aftershock one, statistical features of aftershocks do not depend on the specific definition. Figure 3 shows the rate of aftershocks $\lambda(t)$ as a function of time since the mainshock, which is in good agreement with the hyperbolic time decay predicted by the Omori law, for any distribution $g(f)$ and for different choices of parameters.

In Figure 4, we plot the slip-size distribution $p(n)$ in the synthetic catalog. Results of numerical simulations (Fig. 4) show that for all choices of the distribution $g(f)$ and for different values of parameters, $p(n)$ exhibits a power-law decay. We find the exponent $\eta \simeq 2$ for the Gaussian and exponential $g(f)$. Very interestingly, for a power-law-distributed $g(f)$ and for a wide range of β-values ($\beta \in [3, 8]$), we find $\eta \in [1.6, 1.7]$ corresponding to a b-value close to 1, which is in quantitative agreement with the GR law of instrumental catalogs.

Conclusions

We presented a minimal model for a seismic fault described as a system of two elastically interconnected blocks, with a block representing the fault plane being subject to a random frictional force as opposed to another block having a velocity-strengthening rheology. The evolution of the model presents the typical stick-slip behavior of real fault systems with mainshocks followed by aftershocks distributed in time according to the Omori law. Furthermore, the model reproduces the GR with a realistic b-value when the friction distribution $g(f)$ is a power law. This supports the hypothesis of power-law-distributed Coulomb stress thresholds in agreement with other indications of the self-similar nature of seismic occurrence (Scholz, 2002).

The main difference with previous results is the presence of randomness in the frictional thresholds. This makes the distance to the failure in our model always broadly distributed and allows us to avoid any assumption on the prestress distribution. In our study, indeed, the stress conditions before each slip instability originate from the previous stage of earthquake occurrence. This is a novel result with respect to other scenarios where the Omori decay is obtained only starting from a population of fault patches in which prestresses are uniformly distributed. Assuming the CFC, for instance, the number of faults, which slips in the time interval Δt, is that with $k(u(0) - h(0)) \in [f^{th} - \dot{\tau}(0)\Delta t, f^{th}]$ and is proportional to the stress rate $\dot{\tau}(0)$ for a uniformly distributed $f^{th} - k(u(0) - h(0))$. In particular, under stationary conditions $\dot{\tau}(t) = \text{const}$ this hypothesis gives a steady seismicity rate, whereas the Omori decay is obtained when the stress on the fault increases because of the afterslip relaxation (Perfettini *et al.*, 2005, 2018; Perfettini and Avouac, 2007). In an alternative interpretation (Dieterich, 1994), still assuming that prestresses are uniformly distributed, aftershocks are produced by the response of a population of rate-weakening patches to a coseismic stress change. In the presence of a rate-weakening friction, indeed, the relationship between $\lambda(t)$ and $\dot{u}(t)$ is no further linear (Helmstetter and Shaw,

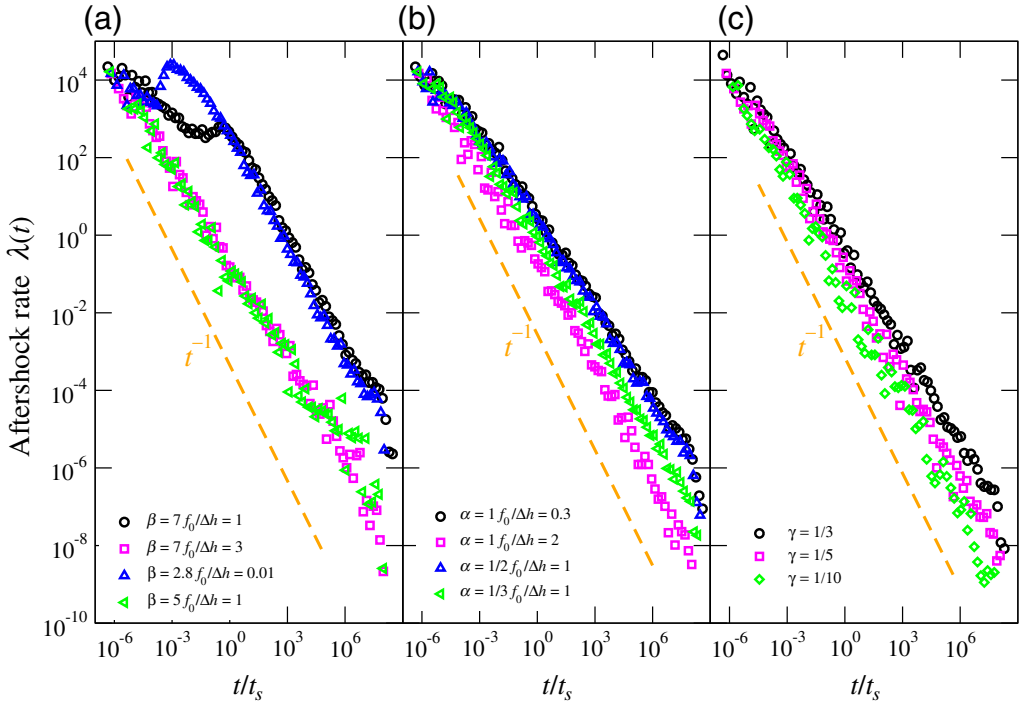

Figure 3. The aftershock rate $\lambda(t)$ as a function of t/t_s, with t the time since the mainshock, for three types of distributions: (a) power law, (b) Gaussian, and (c) exponential. Different symbols correspond to different parameters as in the figure legend. Dashed lines represent the Omori decay $\lambda(t) \sim 1/t$. The color version of this figure is available only in the electronic edition.

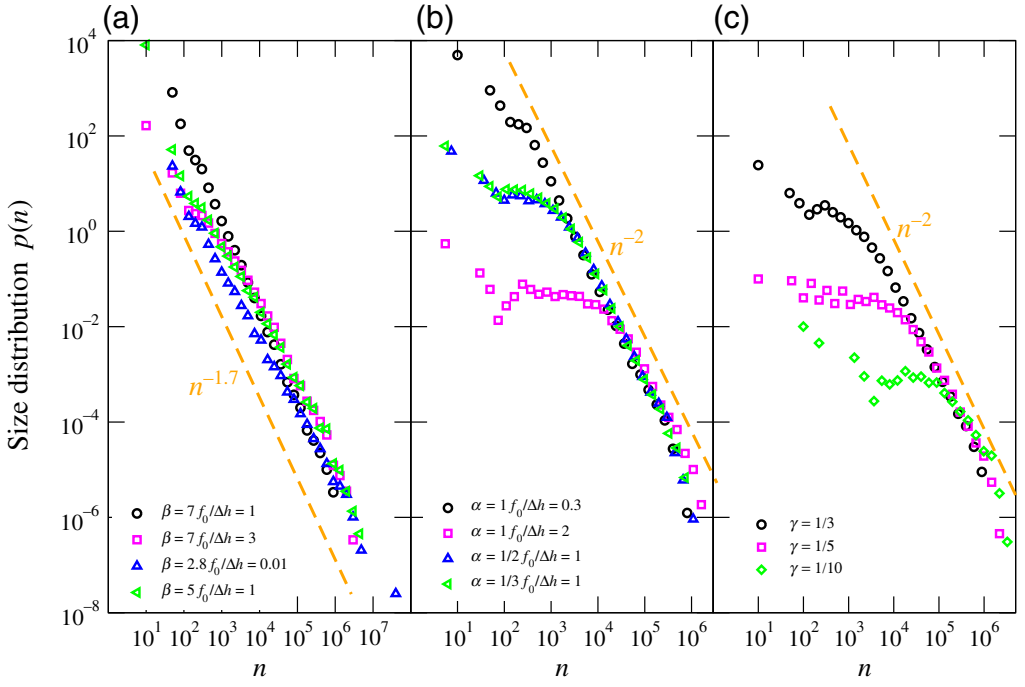

Figure 4. The size distribution $p(n)$ for three types of distributions: (a) power law, (b) Gaussian, and (c) exponential. Different symbols correspond to different parameters as in the figure legend. Dashed lines correspond to the best-fit power-law decay $p(n) \sim n^{-\tau}$. We find $\tau \in (1.6, 1.7)$ for the power law $g(f)$, and $\tau \simeq 2$ for the two other choices of the distribution. The color version of this figure is available only in the electronic edition.

2006) and $\lambda(t)$ decays consistently with the Omori law in response to a stress drop. Savage (2010) has shown that the combination of this relationship, which holds for a velocity-weakening fault (Dieterich, 1994), with the hypothesis that the driving stress is generated by the afterslip evolution (Perfettini and Avouac, 2004) leads to an improved description of postseismic relaxation. A rate-weakening description of the fault block H can be incorporated in our two-block model instead of the more simple CFC. In our approach, we do not include a rate-weakening description of the block H and keep the more simple CFC because it allows us to perform analytical calculations, and at the same time, makes numerical simulations much more simple. Nevertheless, because of heterogeneities in the frictional thresholds and because slip instabilities occur on the instantaneous timescale t_s, details of the friction law acting on the H block are not expected to be relevant. The main effects of the friction laws should reflect in changes of the fault slip Δh, which, however, is not a relevant parameter of our model. Indeed, no significant differences are observed in numerical simulations, in which Δh is not constant but is randomly extracted from a Gaussian distribution.

The comparison with instrumental aftershock sequences would be the subsequent step to support our main conclusions. A further aspect, not investigated in this short note, concerns the understanding of the mechanism leading to the presence of small earthquakes, that is, the foreshocks, which in our numerical simulations anticipate the occurrence of large earthquakes. This could provide new insights on the outstanding question of the nature of foreshocks (de Arcangelis *et al.*, 2016; Lippiello *et al.*, 2017). As a further step, the two-block model can be natural generalized to the many-block Burridge–Knopoff (BK) model (Burrige and Knopoff, 1967) coupled with a velocity-strengthening region. Recent studies (Jagla, 2010; Jagla and Kolton, 2010; Jagla *et al.*, 2014; Lippiello *et al.*, 2015; de Arcangelis *et al.*, 2016; Landes and Lippiello, 2016) have shown that, introducing an intermediate timescale for relaxation in a cellular automata version of the BK model, one recovers statistical features of instrumental catalogs such as the Omori law and the GR law with a realistic b-value. Our results represent a justification for this class of models and provide insights in the mechanisms leading to realistic aftershock features.

Data and Resources

No data were used in this short note.

Acknowledgments

This work was partially supported by the grant from the Simons Foundation, for F. L. (Number 454935 Giulio Biroli, Number 327939 Andrea Liu, and Number 454951 David Reichman).

References

Ader, T. J., N. Lapusta, J.-P. Avouac, and J.-P. Ampuero (2014). Response of rate-and-state seismogenic faults to harmonic shear-stress perturbations, *Geophys. J. Int.* **198,** no. 1, 385–413, doi: 10.1093/gji/ggu144.

Burrige, R., and L. Knopoff (1967). Model and theoretical seismicity, *Bull. Seismol. Soc. Am.* **57,** 341–371.

Canitano, A., M. Godano, Y. Hsu, H. Lee, A. T. Linde, and S. Sacks (2018). Seismicity controlled by a frictional afterslip during a small magnitude seismic sequence ($M_L < 5$) on the Chihshang fault, Taiwan, *J. Geophys. Res.* **123,** no. 2, 2003–2018, doi: 10.1002/2017JB015128.

Crescentini, L., A. Amoruso, and R. Scarpa (1999). Constraints on slow earthquake dynamics from a swarm in central Italy, *Science* **286,** no. 5447, 2132–2134, doi: 10.1126/science.286.5447.2132.

de Arcangelis, L., C. Godano, J. R. Grasso, and E. Lippiello (2016). Statistical physics approach to earthquake occurrence and forecasting, *Phys. Rep.* **628,** 1–91, doi: 10.1016/j.physrep.2016.03.002.

Dieterich, J. (1994). A constitutive law for rate of earthquake production and its application to earthquake clustering, *J. Geophys. Res.* **99,** no. B2, 2601–2618, doi: 10.1029/93JB02581.

Frank, W. B., P. Poli, and H. Perfettini (2017). Mapping the rheology of the central Chile subduction zone with aftershocks, *Geophys. Res. Lett.* **44,** no. 11, 5374–5382, doi: 10.1002/2016GL072288.

Freed, A. M. (2007). Afterslip (and only afterslip) following the 2004 Parkfield, California, earthquake, *Geophys. Res. Lett.* **34,** no. 6, doi: 10.1029/2006GL029155.

Helmstetter, A., and B. E. Shaw (2006). Relation between stress heterogeneity and aftershock rate in the rate-and-state model, *J. Geophys. Res.* **111,** no. B7304, doi: 10.1029/2005JB004077.

Hsu, Y.-J., M. Simons, J.-P. Avouac, J. Galetzka, K. Sieh, M. Chlieh, D. Natawidjaja, L. Prawirodirdjo, and Y. Bock (2006). Frictional afterslip following the 2005 Nias-Simeulue earthquake, Sumatra, *Science* **312,** no. 5782, 1921–1926, doi: 10.1126/science.1126960.

Jagla, E. A. (2010). Realistic spatial and temporal earthquake distributions in a modified Olami-Feder-Christensen model, *Phys. Rev. E* **81,** 046117, doi: 10.1103/PhysRevE.81.046117.

Jagla, E. A., and A. B. Kolton (2010). A mechanism for spatial and temporal earthquake clustering, *J. Geophys. Res.* **115,** no. B5, 312, doi: 10.1029/2009JB006974.

Jagla, E. A., F. P. Landes, and A. Rosso (2014). Viscoelastic effects in avalanche dynamics: A key to earthquake statistics, *Phys. Rev. Lett.* **112,** 174301, doi: 10.1103/PhysRevLett.112.174301.

Johnson, K. M., R. Bürgmann, and K. Larson (2006). Frictional properties on the San Andreas fault near Parkfield, California, inferred from models of afterslip following the 2004 earthquake, *Bull. Seismol. Soc. Am.* **96,** no. 4B, S321, doi: 10.1785/0120050808.

Kaneko, Y., and N. Lapusta (2007). Variability of earthquake nucleation in continuum models of rate-and-state faults and implications for aftershock rates, *J. Geophys. Res.* **113,** no. B12, doi: 10.1029/2007JB005154.

Landes, F. P., and E. Lippiello (2016). Scaling laws in earthquake occurrence: Disorder, viscosity, and finite size effects in Olami-Feder-Christensen models, *Phys. Rev. E* **93,** 051001, doi: 10.1103/PhysRevE.93.051001.

Lippiello, E., F. Giacco, W. Marzocchi, C. Godano, and L. de Arcangelis (2015). Mechanical origin of aftershocks, *Sci. Rep.* **5,** 1–6.

Lippiello, E., F. Giacco, W. Marzocchi, C. Godano, and L. de Arcangelis (2017). Statistical features of foreshocks in instrumental and etas catalogs, *Pure Appl. Geophys.* **174,** 1679–1697, doi: 10.1007/s00024-017-1502-5.

Marone, C. J., C. H. Scholtz, and R. Bilham (1991). On the mechanics of earthquake afterslip, *J. Geophys. Res.* **96,** no. B5, 8441–8452, doi: 10.1029/91JB00275.

Miyazaki, S., P. Segall, J. Fukuda, and T. Kato (2004). Space time distribution of afterslip following the 2003 Tokachi-Oki earthquake: Implications for variations in fault zone frictional properties, *Geophys. Res. Lett.* **31,** no. 6, doi: 10.1029/2003GL019410.

Perfettini, H., and J.-P. Ampuero (2008). Dynamics of a velocity strengthening fault region: Implications for slow earthquakes and postseismic slip, *J. Geophys. Res.* **113,** no. B9, doi: 10.1029/2007JB005398.

Perfettini, H., and J.-P. Avouac (2004). Postseismic relaxation driven by brittle creep: A possible mechanism to reconcile geodetic measurements and the decay rate of aftershocks, application to the Chi-Chi earthquake, Taiwan, *J. Geophys. Res.* **109,** no. B2304, doi: 10.1029/2003JB002488.

Perfettini, H., and J.-P. Avouac (2007). Modeling afterslip and aftershocks following the 1992 Landers earthquake, *J. Geophys. Res.* **112,** no. B7, doi: 10.1029/2006JB004399.

Perfettini, H., J.-P. Avouac, and J.-C. Ruegg (2005). Geodetic displacements and aftershocks following the 2001 $M_w = 8.4$ Peru earthquake: Implications for the mechanics of the earthquake cycle along subduction zones, *J. Geophys. Res.* **110,** no. B9, doi: 10.1029/2004JB003522.

Perfettini, H., W. B. Frank, D. Marsan, and M. Bouchon (2018). A model of aftershock migration driven by afterslip, *Geophys. Res. Lett.* **45,** no. 5, 2283–2293, doi: 10.1002/2017GL076287.

Rice, J. R., and Y. Ben-Zion (1996). Slip complexity in earthquake fault models, *Proc. Natl. Acad. Unit. States Am.* **93,** 3811–3818.

Savage, J. C. (2010). Calculation of aftershock accumulation from observed postseismic deformation: M6 2004 Parkfield, California, earthquake, *Geophys. Res. Lett.* **37,** no. 13, doi: 10.1029/2010GL042872.

Savage, J. C., and J. Langbein (2008). Postearthquake relaxation after the 2004 M6 Parkfield, California, earthquake and rate-and-state friction, *J. Geophys. Res.* **113,** no. B10, doi: 10.1029/2008JB005723.

Savage, J. C., and S.-B. Yu (2007). Postearthquake relaxation and aftershock accumulation linearly related after the 2003 M 6.5 Chengkung, Taiwan, and the 2004 M 6.0 Parkfield, California, earthquakes, *Bull. Seismol. Soc. Am.* **97,** no. 5, 1632, doi: 10.1785/0120070069.

Scholz, C. H. (2002). *The Mechanics of Earthquakes and Faulting*, Cambridge University Press, New York, New York.

E. Lippiello
G. Petrillo
Department of Mathematics and Physics
University of Campania "L. Vanvitelli"
Viale Lincoln 5
81100 Caserta, Italy
eugenio.lippiello@unicampania.it
giuseppe.petrillo@unicampania.it

F. Landes
iPhT
CEA Saclay
91 Orsay
France
francoislandes@gmail.com

A. Rosso
LPTMS, CNRS
Univ. Paris-Sud
Universit-Paris-Saclay
91405 Orsay
France
alberto.rosso@u-psud.fr

Manuscript received 1 September 2018

Queries

1. AU: SSA style requires that author names are not abbreviated. Please provide the full name of all authors.
2. AU: Please note that part labels have been inserted to Figure 1. Kindly check and correct if necessary.
3. AU: Because the figures will only appear in color online, and the text will be the same both online and in print, references to specific colors must be removed throughout the figure captions. Please provide revised wording and/or revised figures as needed.